Heat Shock Protein 70.1 (Hsp70.1) Affects Neuronal Cell Fate by Regulating Lysosomal Acid Sphingomyelinase*

Hong Zhu[‡§], Tanihiro Yoshimoto[§], and Tetsumori Yamashima[‡¶][1]

From the Departments of ‡Restorative Neurosurgery, §Molecular Pharmacology, and ¶Psychiatry and Neurobiology, Kanazawa University Graduate School of Medical Science, 13-1 Takara-machi, Kanazawa, Japan

Background: The role of Hsp70.1 in neurodegeneration remains unknown.

Results: We demonstrate differential profiles in activation of μ-calpain, bis(monoacylglycero)phosphate (BMP) levels, Hsp70.1-BMP interaction, and acid sphingomyelinase (ASM) activity between motor cortex and CA1 after ischemia/reperfusion.

Conclusion: Hsp70.1-mediated ASM activity affects neuronal cell fate by regulating lysosomal membrane stability.

Significance: This finding provides new insights into the mechanism of neuronal death.

The inducible expression of heat shock protein 70.1 (Hsp70.1) plays cytoprotective roles in its molecular chaperone function. Binding of Hsp70 to an endolysosomal phospholipid, bis(monoacylglycero)phosphate (BMP), has been recently shown to stabilize lysosomal membranes by enhancing acid sphingomyelinase (ASM) activity in cancer cells. Using the monkey experimental paradigm, we have reported that calpain-mediated cleavage of oxidized Hsp70.1 causes neurodegeneration in the hippocampal cornu ammonis 1 (CA1), whereas expression of Hsp70.1 in the motor cortex without calpain activation contributes to neuroprotection. However, the molecular mechanisms of the lysosomal destabilization/stabilization determining neuronal cell fate have not been elucidated. To elucidate whether regulation of lysosomal ASM could affect the neuronal fate, we analyzed Hsp70.1-BMP binding and ASM activity by comparing the motor cortex and the CA1. We show that Hsp70.1 being localized at the lysosomal membrane, lysosomal lipid BMP levels, and the lipid binding domain of Hsp70.1 are crucial for Hsp70.1-BMP binding. In the postischemic motor cortex, Hsp70.1 being localized at the lysosomal membrane could bind to BMP without calpain activation and decreased BMP levels, resulting in increasing ASM activity and lysosomal stability. However, in the postischemic CA1, calpain activation and a concomitant decrease in the lysosomal membrane localization of Hsp70.1 and BMP levels may diminish Hsp70.1-BMP binding, resulting in decreased ASM activity and lysosomal rupture with leakage of cathepsin B into the cytosol. A TUNEL assay revealed the differential neuronal vulnerability between the CA1 and the motor cortex. These results suggest that regulation of ASM activation *in vivo* by Hsp70.1-BMP affects lysosomal stability and neuronal survival or death after ischemia/reperfusion.

Acid sphingomyelinase (ASM)[2] (EC 3.14.12) is a glycoprotein that mediates hydrolysis of sphingomyelin to generate cer-

amide and phosphorylcholine. It exists in two enzymatic forms; one is a lysosomal ASM (Zn^{2+}-independent form, simply called ASM here) that is localized predominantly in the lysosomes, whereas the other is the secreted ASM (Zn^{2+}-dependent form) that is released extracellularly (1).

Increasing ASM activity stabilizes lysosomal membranes and promotes survival of cancer cells (2), whereas inhibiting ASM activity in cancer cells could destabilize the lysosomal membranes, thereby increasing non-apoptotic cancer cell death by inhibitors of ASM such as cationic amphiphilic drugs (3) or by anticancer compounds, such as sunitinib (SU11248) and its analog SU11652 (4). It is probable that ASM activity plays a crucial role in the maintenance of lysosomal membrane integrity (5). Interestingly, heat shock protein 70.1 (Hsp70.1; simply Hsp70, also called Hsp72 or HSPA1A), which is expressed in many tumor types, has been highlighted as a key protein that protects lysosomal membranes against destabilization in cancer cells (6, 7). Binding of Hsp70.1 to bis(monoacylglycero)-phosphate (BMP), also called lysobisphosphatidic acid (LBPA), which is an essential co-factor for ASM during lysosomal sphingomyelin hydrolysis (8, 9), enhances ASM activity and promotes lysosomal cell survival by inhibiting lysosomal destabilization (2). Although ASM activity is believed to be involved in regulating lysosomal membrane stability in cancer cells, its role in neuronal cells remains unknown. Using monkeys undergoing transient global brain ischemia, the role of lysosomal rupture in programmed neuronal necrosis has been grossly elucidated by the "calpain-cathepsin hypothesis" that was formulated by Yamashima and colleagues (10–13). Recently, we have demonstrated that calpain-mediated cleavage of oxidized Hsp70.1 in the hippocampal cornu ammonis 1 (CA1) can induce lysosomal rupture and neurodegeneration (14, 15), whereas up-regulation of Hsp70.1 in the motor cortex contributes to neuroprotection (16).

The aim of this study was to reveal the molecular mechanisms underlying *in vivo* Hsp70.1-affected lysosomal membrane integrity and neuronal cell fate by regulating ASM

---

[1] To whom correspondence should be addressed. Tel.: 81-76-265-2381; Fax: 81-76-234-4264; E-mail: yamashima215@gmail.com.

[2] The abbreviations used are: ASM, acid sphingomyelinase; CA1, cornu ammonis 1; BMP, bis(monoacylglycero)phosphate; LBPA, lysobisphospha-

tidic acid; LAMP1 to -3, lysosome-associated membrane proteins 1–3; PCC, Pearson's correlation coefficient; MCC, Mander overlap coefficient.

activation using the same ischemic monkey experimental paradigms.

EXPERIMENTAL PROCEDURES

Animals—All experimental procedures were performed in strict adherence with the guidelines of the Animal Care and Ethics Committee of Kanazawa University and the National Institutes of Health Guide for the Care and Use of Laboratory Animals. Thirty Japanese monkeys (*Macaca fuscata*) with a body weight of 5–10 kg were bred in air-conditioned cages and allowed free daily access to food and water. Under general anesthesia, transient global brain complete ischemia was made by clamping the innominate and left subclavian arteries for 20 min, according to the procedure previously described (17), whereas the control monkeys underwent a sham operation. After the operation, two experimental groups including the control and the postischemic day 3, 5, 7, and 9 monkeys were sacrificed (each time point includes 3 monkeys, $n = 15$ for each group). One group was used for the immunofluorescence analysis, whereas another group was used for Western blot and ELISA.

Immunofluorescent Analysis—For the histological analysis, the brains were perfused with 0.5 liter of ice-cold saline followed by 1 liter of 4% paraformaldehyde and fixed in 4% paraformaldehyde for 2 weeks. Then the motor cortex and hippocampal tissues were cryoprotected in 30% sucrose and cut into cryosections of 30-μm thickness. Free floating frozen sections (control, postischemic days 3–9 for both motor cortex and hippocampus) were used for the signal and double immunofluorescent staining. First, the sections were washed twice with phosphate-buffered saline (PBS) and permeabilized with 0.5% Tween 20 in PBS for 15 min at room temperature. To block nonspecific bindings, the sections were incubated for 30 min at room temperature with 10% goat serum (Vector Laboratories, Burlingame, CA), 1% bovine serum albumin (BSA) in PBS. Subsequently, they were incubated for 48 h at 4 °C with the following primary antibodies: anti-Hsp70.1 diluted at 1:100 (Enzo Life Sciences, Plymouth Meeting, PA), anti-CD63 at 1:50, or anti-ceramide at 1:100 (Life Span Bio Sciences, Seattle, WA), anti-lysobisphosphatidic acid (6C4) (product number Z-SLBPA, also termed BMP) at 1:50 (Echelon Biosciences, Salt Lake City, UT), anti-lysosome-associated membrane protein 1 (LAMP1) at 1:200, anti-ASM at 1:200 (Abcam, Cambridge, MA), anti-activated form of human μ-calpain at 1:50 (18). After the sections were washed three times with PBS, they were finally incubated for 2 h at room temperature with secondary antibodies, such as goat anti-rabbit IgG or anti-mouse IgG/IgM conjugated with Alex Fluor 488 or 546 (Invitrogen). Then the stained sections were mounted on the glass slides by Vectashield mounting medium (Vector Laboratories, Burlingame, CA). Slides were observed using a laser confocal microscope (LSM510, Carl Zeiss). The negative controls were made by omitting the respective primary antibodies. Quantification of the fluorescent intensity and colocalization analysis was carried out with LSM 510 META software. Background was corrected in manual mode using the selected region of interest (ROI). Quantitative colocalization was estimated by calculating colocalization coefficients (Pearson's correlation coefficients and overlap coefficients according to Mander). A Pearson's correlation coefficient (PCC) value of >0.5 and an overlap coefficient according to Mander (MOC) value of >0.6 indicate colocalization (19).

Isolation of Lysosomal and Cytosolic Fractions from the Motor Cortex and CA1—The cytosolic and enriched lysosomal fractions were prepared using a lysosome enrichment kit for tissue and cultured cells (Thermo Scientific) with some modifications as described in detail (20).

ELISA—The concentrations of Hsp70.1 and ASM were measured by the HSP70 ELISA kit (Enzo Life Sciences, Plymouth Meeting, PA) or human ASM ELISA kit (CUSABIO, Tokyo, Japan) according to the manufacturer's instructions. The intensity of color was measured in a microplate reader (Sunrise Tecan, Wako, Japan) at 450 nm. The concentrations of Hsp70 and ASM from the samples were quantitated based on the standard curve and expressed as ng/mg of total protein.

TUNEL Assay—DNA fragmentation was detected on cryosections using the ApopTag Plus Fluorescein *in situ* apoptosis detection kit (Millipore) as described previously (16).

Western Blot—The lysosome or the cytosol lysate was separated by 10–12% SDS-polyacrylamide gel electrophoresis, and membranes were transferred to a Trans-Blot Turbo transfer pack according to the manufacturer's instructions (Bio-Rad). Then membranes were blocked for 1 h at room temperature with 10% (w/v) nonfat dry milk in 0.02 mol/liter Tris-HCl, pH 7.4, containing 0.136 mol/liter NaCl and 0.1% Tween 20 and incubated overnight at 4 °C by the following primary antibodies: anti-Hsp70 at a dilution of 1:1000 (Enzo Life Science), anti-human Hsp70 (C-terminal) at 1:1000 (Epitomics, Burlingame, CA), anti-histone H1 at 1:3000 (Active Motif, Carlsbad, CA), anti-calreticulin at 1:1000 (Life Span Bio Sciences, Seattle, WA), anti-Golgin-84 at 1:1000 (Santa Cruz Biotechnology, Inc., Dallas, Texas), anti-ASM at 1:1000, anti-cathepsin B (ABcam, Tokyo, Japan) at 1:1000, anti-LAMP1 at 1:1000, and anti-GAPDH at 1:3000 (Abcam). Membranes were washed before incubation with a horseradish peroxidase-conjugated antibody. ECL chemiluminescence (Amersham Biosciences) was used to visualize bands according to the manufacturer's instructions.

Statistical Analysis—Data in all figures are expressed as mean $\pm$ S.E. The data are means of three separate experiments. The density of protein bands was analyzed and quantification of the fluorescence intensity was performed using ImageJ image analysis software. Statistical significance was determined by one-way analysis of variance with Bonferroni or Dunnet tests, using GraphPad Prism 6 (Oberlin, San Diego, CA). A two-tailed $p < 0.05$ was considered statistically significant. Positive cells for TUNEL were evaluated in grids of 800×1000 μm.

RESULTS

Assaying Lysosome/Cytosol Purification—To assess whether the procedure can isolate the enriched lysosomal or cytosolic fraction, the collected fractions from the motor cortex, including the non-ischemic control and postischemic days 3, 5, 7, and 9, were subjected to Western blot with the markers of subcellular organelles. Fig. 1*A* shows that a lysosomal marker, LAMP1, was highly enriched in the lysosomal fraction isolated from the motor cortex without a cytoplasmic marker, GAPDH,
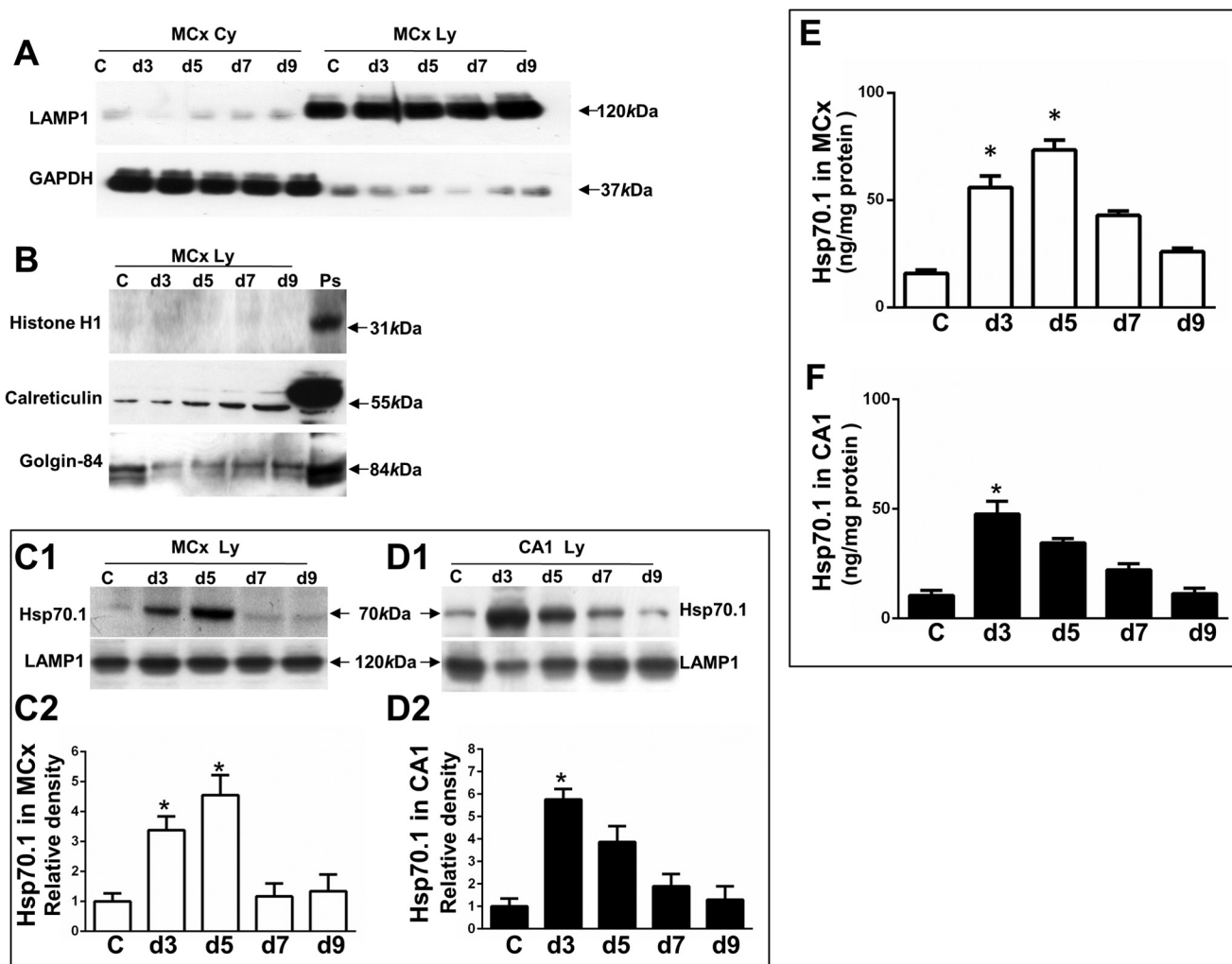
FIGURE 1. **Purification of enriched lysosomal fraction and determining inducible Hsp70.1 in this fraction.** The collected cytosolic fraction (*MCx Cy*) and lysosomal enriched fraction (*Mcx Ly*), including the non-ischemic control and postischemic days from the motor cortex, were confirmed by the presence of organelle marker proteins, as indicated by anti-LAMP1 for a lysosomal marker protein, anti-GAPDH for a cytoplasmic marker protein, anti-histone H1 for a nuclear marker protein, anti-calreticulin for an endoplasmic reticulum marker protein, and anti-Golgin-84 for a Golgi marker protein. *C*, non-ischemic control. *d3*, *d5*, *d7*, and *d9*, postischemic days 3, 5, 7, and 9. *Ps*, a positive control. *A*, the lysosome-enriched fraction was confirmed by LAMP1, whereas the cytosolic fraction was confirmed by GAPDH. *Arrows*, a band of LAMP1 at 120 kDa and GAPDH at 37 kDa. *B*, the lysosome-enriched fraction did not contain histone H1 but did contain calreticulin and Golgin-84. Positive controls were collected from the nuclear fraction of the non-ischemic monkey motor cortex for detecting nuclear protein or from the rat brain lysate for detecting endoplasmic reticulum and Golgi. *Arrows*, a band of histone H1 at 31 kDa, calreticulin at 55 kDa, and Golgin-84 at 84 kDa. *C1* and *D1*, Western blot showing Hsp70.1 in lysosome-enriched fractions, including the non-ischemic control and postischemic days 3–9 from the motor cortex and CA1 (*CA1 Ly*). *Arrows*, Hsp70.1 band at 70 kDa and LAMP1 at 120 kDa. *C2* and *D2*, densitometric analysis of Hsp70.1 in the postischemic motor cortex and CA1 as compared with the non-ischemic control. *E* and *F*, ELISA showing Hsp70.1 concentrations in the lysosome-enriched fractions, including the non-ischemic control and postischemic days 3–9 from motor cortex (*white bars*) and CA1 (*black bars*). Lysosomal fractions with recombinant Hsp70 standards were incubated with an anti-Hsp70 immunoassay plate. Hsp70.1 concentrations were calculated based on the standard curve and expressed as ng of Hsp70/1 mg of total proteins. The values represent mean ± S.E. from three independent experiments. *Asterisks* show significant difference from the non-ischemic control (*, $p < 0.05$). All experiments were repeated three times with similar results.

whereas GAPDH was highly enriched in the cytosolic fraction without LAMP1. Fig. 1*B* shows that lysosomal fraction did not contain a nuclear fraction marker, histone H1, but this fraction contained an endoplasmic reticulum marker, calreticulin, as well as a Golgi apparatus marker, Golgin-84. This procedure is also suitable for obtaining a lysosomal or cytosolic fraction isolated from CA1 with a similar result (data not shown).

Up-regulation of Hsp70.1 in the Enriched Lysosomal Fraction—To determine whether ischemia/reperfusion can induce up-regulation of Hsp70.1 in the motor cortex and CA1, we first quantified the inducible Hsp70.1 in the lysosome-enriched fraction including postischemic days 3–9 as compared with the non-ischemic control by Western blot with densitometric anal-

ysis. A significant increase in expression of Hsp70.1 was found in the lysosome-enriched fraction from postischemic motor cortex days 3 and 5, by 3.3- and 4.7-fold, respectively, as compared with the non-ischemic control (Fig. 1, *C1* and *C2*). Similarly, a significant increase in expression of Hsp70.1 was found in the lysosome-enriched fraction from postischemic CA1 days 3 and 5, by 5.7- and 3.8-fold, respectively, as compared with the non-ischemic control (Fig. 1, *D1* and *D2*). Next, we measured Hsp70 concentrations in the lysosome-enriched fraction by ELISA and found a significant increase in Hsp70.1 concentrations in the lysosome-enriched fraction from postischemic motor cortex days 3 and 5 by 3.5- and 4.5-fold, respectively, compared with the non-ischemic control (Fig. 1*E*) as well as a
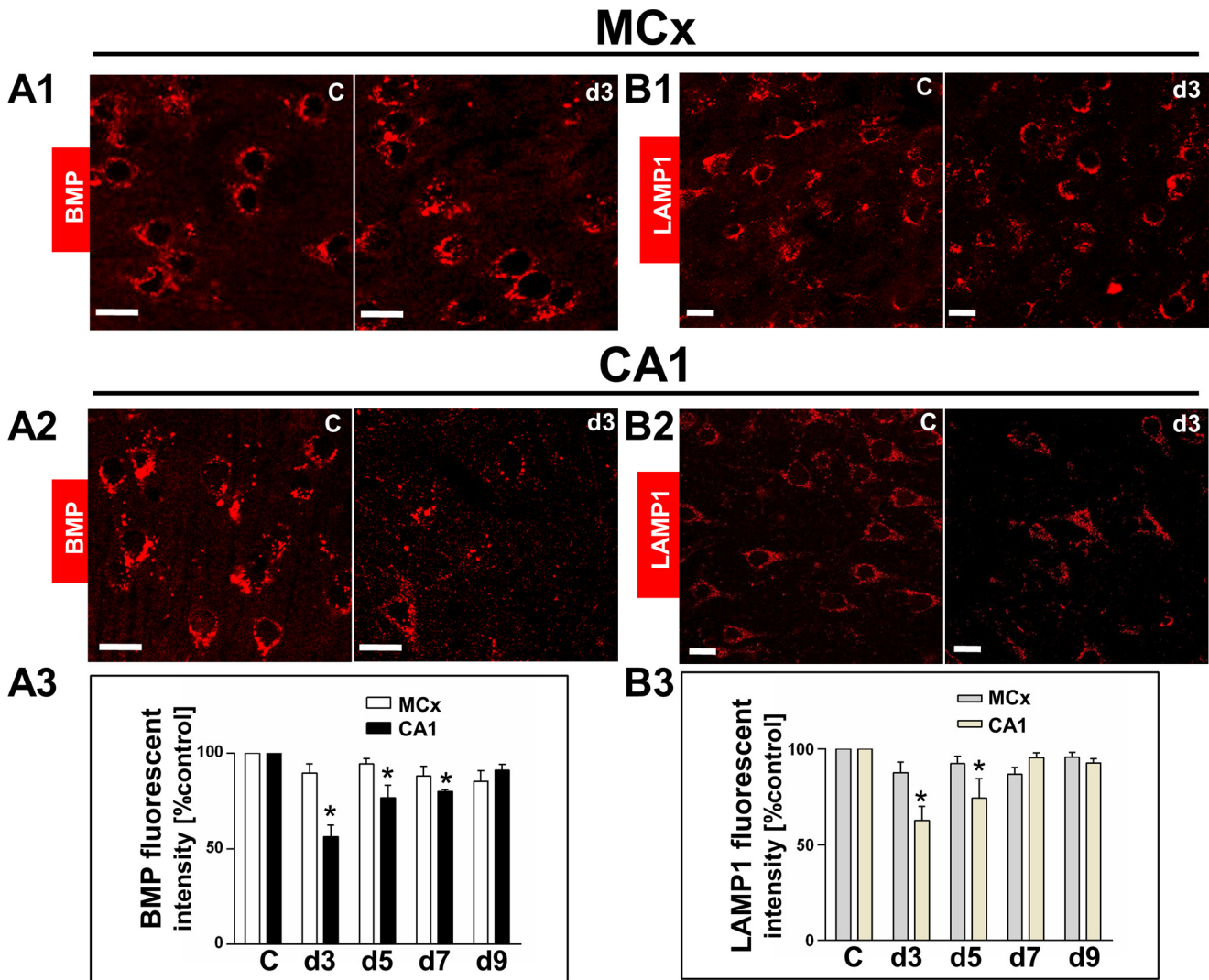
FIGURE 2. **Analysis of BMP levels and lysosomal membrane protein LAMP1 levels in motor cortex and CA1.** Lysosomal lipid (BMP) and lysosomal membrane protein (LAMP1) levels were measured by quantifying fluorescent intensity using antibodies against BMP (LBPA) and LAMP1. *MCx*, motor cortex. *C*, non-ischemic control. *d3*, *d5*, *d7*, and *d9*, postischemic days 3, 5, 7, and 9. *A1* and *A2*, comparison of the BMP fluorescent intensity between the non-ischemic control and at postischemic day 3 from motor cortex and CA1. *A3*, quantitative analysis showing that BMP levels were unchanged in the postischemic motor cortex, whereas they were decreased in the postischemic CA1 at days 3–7 as compared with the non-ischemic control. *B1* and *B2*, comparison of LAMP1 fluorescent intensity between the non-ischemic control and at postischemic day 3 from motor cortex and CA1. *B3*, quantitative analysis showing that LAMP1 levels were unchanged in the postischemic motor cortex, whereas they were decreased in postischemic CA1 at days 3 and 5 as compared with the non-ischemic control. The values represent mean ± S.E. from three independent experiments. *Asterisks* show significant difference from the non-ischemic control (*, $p < 0.05$). *Scale bar*, 20 μm.

significant increase in Hsp70.1 concentrations in the lysosome-enriched fraction from postischemic CA1 day 3 by 3.1-fold, compared with the non-ischemic control (Fig. 1*F*).

Determination of LAMP1 and BMP Levels—As in the above observation by Western blot, a significant decrease in LAMP1 proteins from lysosomal fraction was observed in the postischemic CA1 day 3 but not in the postischemic motor cortex. To further confirm this, lysosomal lipid BMP levels and the lysosomal membrane protein LAMP1 were assessed by immunofluorescence staining, compared with the non-ischemic control. The BMP levels remained unchanged in the postischemic motor cortex, compared with the non-ischemic control (Fig. 2, *A1* and *A3*), whereas they were significantly reduced in the postischemic CA1 at days 3, 5, and 7 by 44, 30 and 25%, respectively, compared with the non-ischemic control (Fig. 2, *A2* and *A3*). The postischemic motor cortex showed unchanged

LAMP1 levels (Fig. 2, *B1* and *B3*), whereas the postischemic CA1 at days 3 and 5 showed a significant decrease by 35 and 21%, respectively, compared with the non-ischemic control (Fig. 2, *B2* and *B3*).

Hsp70.1 Can Bind with BMP in the Postischemic Motor Cortex Devoid of Calpain Activation—We have recently reported that up-regulation of Hsp70.1 was colocalized with lysosome-associated membrane proteins 1 and 2 (LAMP1 and LAMP2) in postischemic motor cortex where activated μ-calpain could not be detected by Western blot coupled with activated μ-calpain-positive controls from the same monkey (16). Because the process producing brain injury involves a complex series of pathophysiological events, during the surgery for monitoring and for producing ischemia, monkeys exhibited physiological or injury variability. In order to confirm whether Hsp70.1 is localized to the lysosomal membranes in current ischemic monkey models,
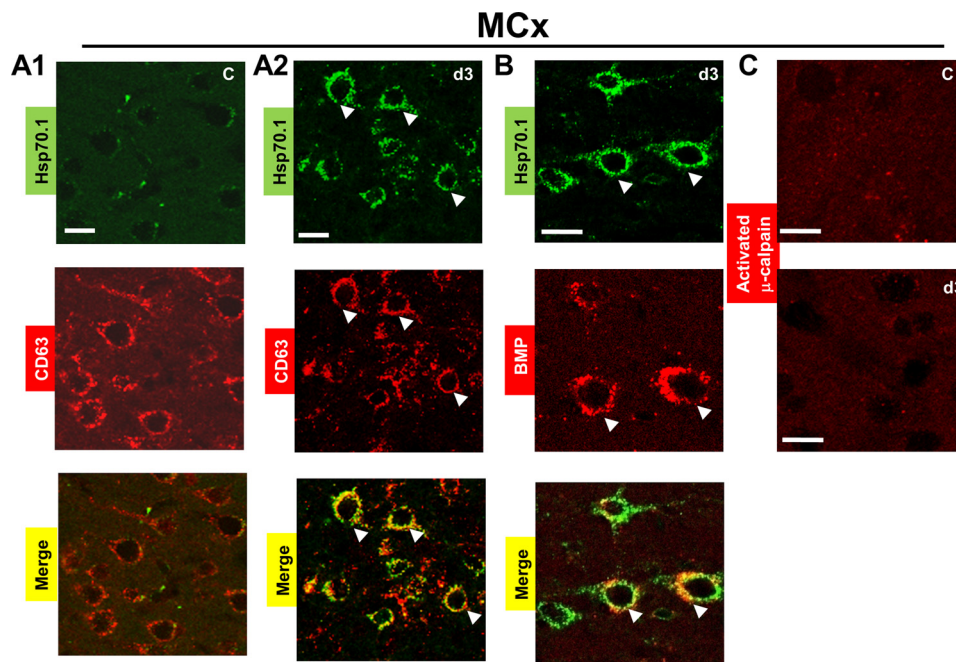
FIGURE 3. **Hsp70.1 is localized to lysosomal membranes and binds with BMP in the postischemic motor cortex, where activated μ-calpain could not be detected.** Frozen sections, including the non-ischemic control and the postischemic day 3 motor cortex, were double-labeled with Hsp70 antibody (*green signal*) and CD63 antibody (*red signal*) or BMP (LBPA) antibody (*red signal*). The *arrows* indicate colocalization (*yellow signal*) based on the colocalization coefficients. *MCx*, motor cortex. *C*, non-ischemic control. *d3*, postischemic day 3. *A1*, clear absence of colocalization of Hsp70.1 and CD63 in the non-ischemic control. *A2*, colocalization of Hsp70.1 and CD63 at postischemic day 3. *B*, colocalization of Hsp70.1 and BMP (LBPA) at postischemic day 3. *C*, immunofluorescence staining of the motor cortex using anti-human activated μ-calpain antibody (*red signal*) demonstrates that μ-calpain activation was not detected either in the non-ischemic control or at postischemic day 3. All experiments were repeated three times with essentially similar results. *Scale bar*, 20 μm.

here we double-labeled Hsp70.1 with CD63, which is also abundantly present in late endosomes/lysosomes, also known as lysosome-associated protein 3 (LAMP3). In the non-ischemic control, the green fluorescence of Hsp70.1 (*green image* in Fig. 3*A1*) could not be detected; thus, quantitative analysis revealed the absence of colocalization of Hsp70.1 and CD63 (*overlay image* of *green* and *red* in Fig. 3*A1*, correlation coefficients of 0.23 ± 0.03 (PCC) and 0.39 ± 0.06 (MOC)) as well as the absence of colocalization of Hsp70.1 and BMP (data not shown). In postischemic day 3, Hsp70.1 green fluorescence became intense in neurons (*green image* in Fig. 3*A2*). Quantitative measure of colocalization as compared with the non-ischemic control revealed a high degree of colocalization between Hsp70.1 and CD63 (*overlay image* of *green* and *red* in Fig. 3*A2*, correlation coefficients of 0.58 ± 0.04 (PCC) and 0.89 ± 0.08 (MOC)). We asked whether the lysosomal membrane localization of Hsp70.1 could interact or bind to lysosomal lipid, BMP. As shown in Fig. 3*B*, we observed colocalization of Hsp70.1 and BMP in postischemic day 3 (correlation coefficients of 0.61 ± 0.03 (PCC) and 0.92 ± 0.05 (MOC)). We also observed a similar result, using an anti-BMP monoclonal antibody (6C4; 1 mg/ml) (21). To further investigate calpain activation, immunofluorescence staining was performed with the same μ-calpain antibody used for Western blot. As shown in Fig. 3*C*, μ-calpain activation was not detected in the motor cortex, including the non-ischemic control, at postischemic day 3 and other ischemic time points (data not shown).

Hsp70.1 Fails to Bind with BMP in the Postischemic CA1 with Calpain Activation—Previous studies have shown that the increase of activated μ-calpain occurs from 3 h after ischemia

until day 5 in CA1 (10). As shown in Fig. 4*A*, activated μ-calpain was detected in postischemic day 3, whereas it could not be detected in non-ischemic control. Notably, calpain was colocalized with LAMP1 in postischemic CA1 (Fig. 4*B*, correlation coefficients of 0.63 ± 0.04 (PCC) and 0.86 ± 0.03 (MOC)), suggesting its effects on the lysosomal membranes. Here, we hypothesized that the presence of activated μ-calpain at lysosomes associated with decreases in the LAMP1 levels and BMP levels could affect Hsp70.1 binding with BMP. To test this hypothesis, we measured the colocalization of Hsp70 in the non-ischemic control and postischemic days. First, we found that the non-ischemic control displayed the absence of colocalization of Hsp70 with LAMP1, CD63, and BMP because Hsp70.1 could not be detected here (data not shown). Next, we found that the postischemic CA1 displayed intense Hsp70.1 green fluorescence in pyramidal neurons (*green image* in Fig. 4, *C1*, *C2*, and *D*) but a low degree of colocalization of Hsp70.1 and LAMP1 (Fig. 4*C1*, correlation coefficients of 0.34 ± 0.06 (PCC) and 0.47 ± 0.03 (MOC)) as well as a low degree of colocalization of Hsp70.1 and CD63 (Fig. 4*C2*, correlation coefficients of 0.48 ± 0.08 (PCC) and 0.55 ± 0.05 (MOC)), as compared with the non-ischemic control. Finally, we found that postischemic CA1 displayed an absence of colocalization of Hsp70.1 and BMP (Fig. 4*D*, correlation coefficients 0.18 ± 0.02 (PCC) and 0.38 ± 0.03 (MOC)) as compared with the non-ischemic control.

The Presence or Absence of Hsp70-BMP Interaction Differentially Regulates ASM in the Postischemic Motor Cortex and CA1—To investigate whether the Hsp70-BMP interaction can regulate expression of ASM, we measured its concentrations in
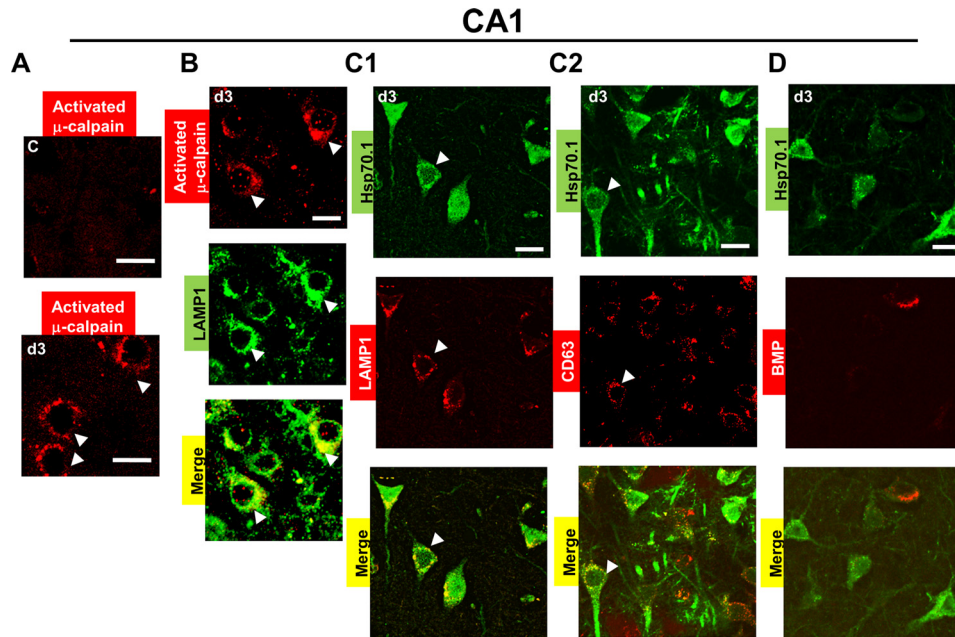
FIGURE 4. **Hsp70.1 is unable to bind with BMP in the postischemic CA1 where μ-calpain was activated.** Frozen CA1 sections were double-labeled with Hsp70 antibody (*green signal*), LAMP1 (*red signal*), CD63 antibody (*red signal*), and BMP antibody (*red signal*). *Arrows*, activated μ-calpain or colocalization (*yellow signal*) based on the colocalization coefficients. *C*, non-ischemic control. *d3*, postischemic day 3. *A*, immunofluorescence staining using activated μ-calpain antibody (*red signal*) showing μ-calpain activation at postischemic day 3 as compared with the non-ischemic control. *B*, double labeling of LAMP1 (*green signal*) and activated μ-calpain (*red signal*) showing colocalization of activated μ-calpain with the lysosomes at postischemic day 3. *C1* and *C2*, a low degree of colocalization between Hsp70.1 and LAMP1 as well as between Hsp70.1 and CD63 at postischemic day 3. *D*, the absence of colocalization between Hsp70.1 and BMP (LBPA) at postischemic day 3. All experiments were repeated three times with essentially similar results. *Scale bar*, 20 μm.
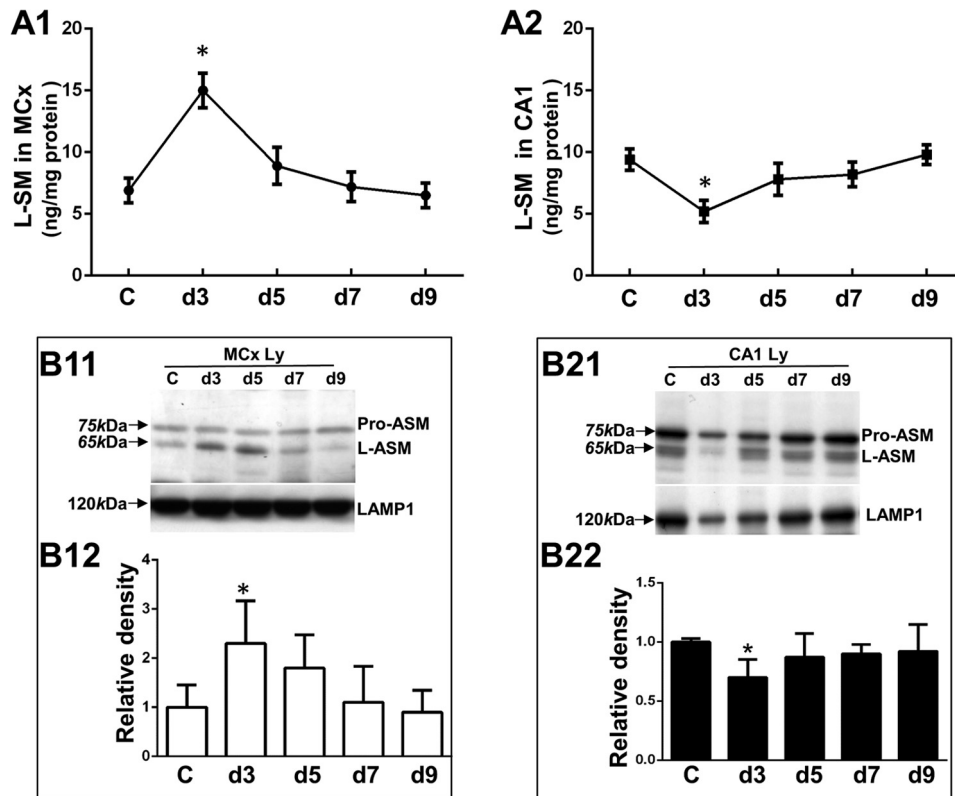

FIGURE 5. **Analysis of lysosomal acid sphingomyelinase protein expression in the postischemic motor cortex and CA1.** *C*, non-ischemic control. *d3*, *d5*, *d7*, and *d9*, postischemic days 3, 5, 7, and 9. *A1* and *A2*, ELISA showing the concentrations of ASM proteins in the lysosome-enriched fractions, including the non-ischemic control and postischemic days 3–9 from the motor cortex (*L-SM in MCx*) or CA1 (*L-SM in CA1*). *B11* and *B21*, Western blot analysis showing ASM proteins in the lysosome-enriched fractions, including the non-ischemic control and postischemic days 3–9 from the motor cortex (*MCx Ly*) or CA1 (*CA1 Ly*) with LAMP1 as a loading control. The *arrows* indicate the band of proform acid sphingomyelinase (*pro-ASM*) at 75 kDa, the band of human mature ASM form (*L-ASM*) at 65 kDa, and the LAMP1 band at 120 kDa. *B12* and *B22*, densitometric analysis of expression of ASM proteins in the motor cortex or CA1 as compared with the density of the non-ischemic control. The values represent mean ± S.E. from three independent experiments. *Asterisks*, significant difference from the non-ischemic control (*, $p < 0.05$). All experiments were repeated three times with similar results.
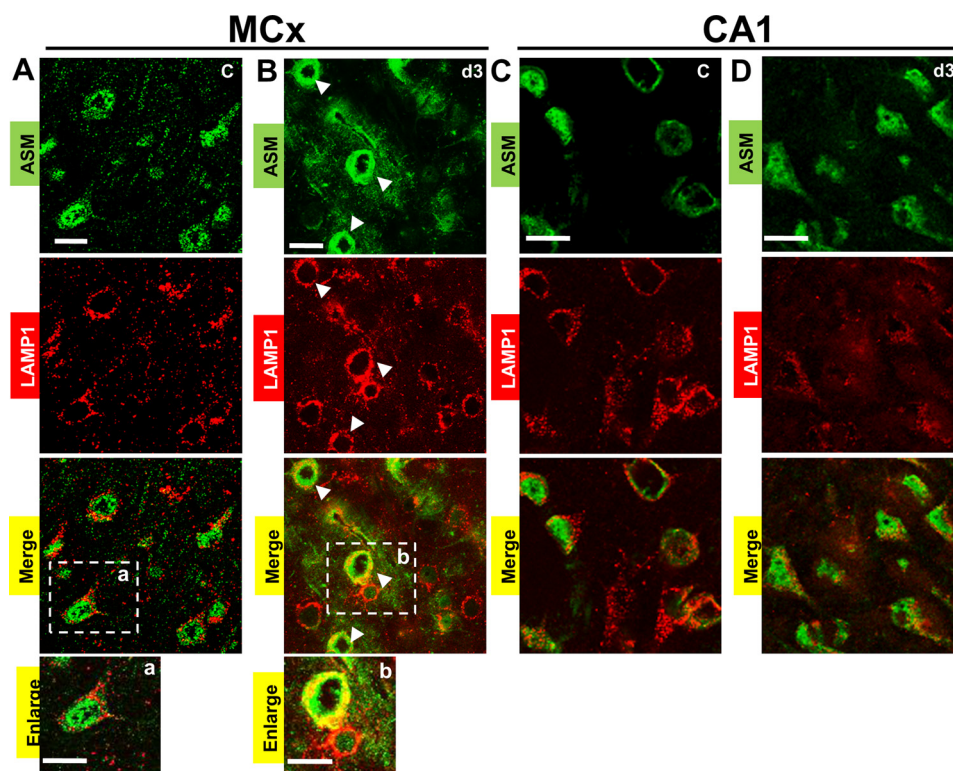
FIGURE 6. **Acid sphingomyelinase (*ASM*) is localized to lysosomes in the postischemic motor cortex but not in the postischemic CA1.** Double labeling of ASM (*green signal*) and a lysosomal marker, LAMP1 (*red signal*), was remarkably seen in the day 3 motor cortex but was negligible in CA1. *MCx*, motor cortex. *C*, non-ischemic control. *d3*, postischemic day 3. *a* and *b*, *enlarged images* of the *boxed areas*. *A*, absence of colocalization between ASM and the lysosomes in the non-ischemic control motor cortex. *B*, colocalization of ASM and the lysosomes in the postischemic day 3 motor cortex. *Arrows*, colocalization (*yellow signal*) based on colocalization coefficients. *C* and *D*, the absence of colocalization between ASM and the lysosomes in the non-ischemic control CA1 and the postischemic day 3 CA1. *Scale bar*, 20 μm.

the enriched lysosome fraction using ELISA. The postischemic day 3 motor cortex showed an increase in ASM concentrations by 2.1-fold, compared with the non-ischemic control (Fig. 5*A1*). In contrast, the postischemic day 3 CA1 showed a 52% decrease, compared with the non-ischemic control (Fig. 5*A2*). ASM concentrations in both the postischemic motor cortex and postischemic CA1 returned to the basal levels after the postischemic day 5 (Fig. 5, *A1* and *A2*). ASM is known to be processed from a 75-kDa, Zn^{2+}-activated proenzyme to a mature 65-kDa, Zn^{2+}-independent form (22). Western blot analysis showed a 2.3-fold increase in the mature human ASM expression (65 kDa) in the postischemic day 3 motor cortex, as compared with the non-ischemic control (Fig. 5, *B11* and *B12*). On the other hand, a 40% decrease in its expression was found in the postischemic day 3 CA1, compared with the non-ischemic control (Fig. 5, *B21* and *B22*). Furthermore, we double-labeled ASM with LAMP1, confirming that the increased ASM was localized at lysosomes in the postischemic day 3 motor cortex (Fig. 6*B*, correlation coefficients 0.59 ± 0.08 (PCC) and 0.82 ± 0.07 (MOC)). We could not find lysosomal membrane localization of ASM in the non-ischemic motor cortex (Fig. 6*A*, correlation coefficients of 0.23 ± 0.04 (PCC) and 0.36 ± 0.03 (MOC)) in the non-ischemic CA1 (Fig. 6*C*, correlation coefficients 0.34 ± 0.02 (PCC) and 0.47 ± 0.03 (MOC)) and in the postischemic day 3 CA1 (Fig. 6*D*, correlation coefficients 0.28 ± 0.06 (PCC) and 0.49 ± 0.04 (MOC)).

To address whether the increase or decrease in the expression of ASM proteins correlates with the changes of its enzyme activity, the ASM activity *in vivo* was assessed by the colocalization of ASM and BMP because the presence of anionic lipids, such as BMP, can stimulate ASM activity (8, 23, 24). ASM colocalization with BMP was detected in the postischemic day 3 motor cortex (Fig. 7*B*, correlation coefficients 0.59 ± 0.04 (PCC) and 0.86 ± 0.03 (MOC)) but was not detected in the non-ischemic control (Fig. 7*A*, correlation coefficients 0.38 ± 0.07 (PCC) and 0.45 ± 0.02 (MOC)) and other postischemic time points (data not shown).

ASM activation leads to hydrolysis of sphingomyelin and generation of ceramide. To further assess the intracellular ASM activation, we measured generation of ceramide by immunofluorescence staining using anti-ceramide antibody. As shown in Fig. 7*C*, ceramide was localized at the membrane bilayer in postischemic day 3 motor cortex but not in the non-ischemic control. Colocalization of ceramide and LAMP1 (Fig. 7*D2*, correlation coefficients of 0.68 ± 0.03 (PCC) and 0.82 ± 0.05 (MOC)) indicated that ceramide was localized at lysosomal membranes of the postischemic motor cortex at day 3. The colocalization of ceramide with a plasma membrane marker, wheat germ agglutinin, could not be detected (Fig. 7*D1*, correlation coefficients of 0.28 ± 0.05 (PCC) and 0.40 ± 0.03 (MOC)), suggesting that ceramide was not mobilized to the plasma membranes. In contrast, the fluorescent intensity of ceramide showed a decrease in postischemic CA1 at day 3, compared with the non-ischemic control (Fig. 7, *E1* and *E2*). The result suggested a decrease in ASM activity with a concomitant decrease in ceramide.
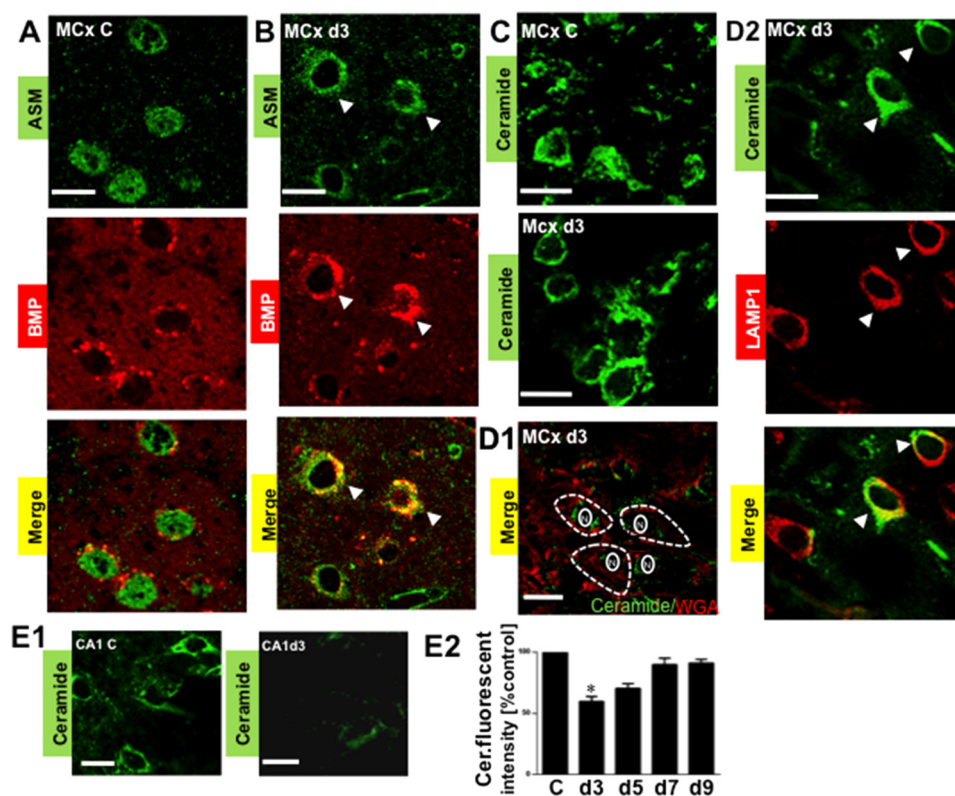
FIGURE 7. **Analysis of ASM activity in the postischemic motor cortex and CA1.** The activity of ASM was assessed by colocalization of ASM and BMP, which is an essential co-factor for facilitating ASM activity. *A*, the absence of colocalization between ASM and BMP in the non-ischemic control motor cortex (*MCx C*). *B*, colocalization of ASM and BMP in postischemic day 3 motor cortex (*MCx d3*). *Arrows*, colocalization (*yellow signal*) based on colocalization coefficients. *C*, confocal microcopy analysis using ceramide antibody (*green signal*), showing a change in the cellular distribution of ceramide in the postischemic day 3 motor cortex as compared with the non-ischemic control motor cortex. *D1*, double labeling of ceramide antibody (*green signal*) with a plasma membrane marker, wheat germ agglutinin (*WAG, red signal*) in postischemic day 3 motor cortex. The absence of colocalization indicates that ceramide was not mobilized to the plasma membranes. The *white interrupted line* is used to define the plasma membrane, whereas the *solid white line* is used to define the nuclear membrane. *N*, nuclear. *D2*, colocalization of ceramide (*green signal*) and lysosomes (LAMP1; *red signal*) indicates that activation of ASM led to the generation of the lysosomal ceramide in postischemic day 3 motor cortex (*MCx d3*). *Arrows*, colocalization (*yellow signal*) based on colocalization coefficients. *E1*, confocal microcopy analysis of ceramide levels using ceramide antibody (*green signal*) in the non-ischemic control CA1 (*CA1 C*) and the postischemic day 3 CA1 (*CA1 d3*). *E2*, quantitative analysis showing that ceramide levels were decreased in the postischemic CA1 at day 3. *C*, non-ischemic control. *d3, d5, d7*, and *d9*, postischemic days 3, 5, 7, and 9. The values represent the mean ± S.E. (*error bars*) of three independent experiments. *Asterisks* show significant difference from the non-ischemic control (*, $p < 0.05$). *Scale bar*, 20 μm.

Differential Regulation of ASM Leads to the Distinct Neuronal Cell Fate—To further investigate whether the increase in ASM activity is responsible for the lysosomal stabilization and neuronal cell survival, we measured the extent of the cathepsin B leakage. Mature cathepsin B was found equally distributed in the lysosomal fraction of the motor cortex at each ischemic time point (Fig. 8, *A1* and *A3*). It was not detected in cytoplasm (Fig. 8, *A2* and *A3*). In contrast to the motor cortex, the cathepsin B in the lysosomal fraction was decreased by 20 and 44% (Fig. 8, *B1* and *B3*) with a concomitant increase in the cytosol fraction by 2.0- and 2.6-fold (Fig. 8, *B2* and *B3*) at postischemic days 3 and 5 CA1 as compared with the non-ischemic control. These results indicated that lysosomal membrane destabilization followed by relocalization cathepsin B from lysosomes into the cytosol occurred in the postischemic CA1 but not in postischemic motor cortex. Lysosomal membrane destabilization can induce cell death, as determined by a TUNEL assay. Compared with its respective non-ischemic control, the motor cortex (Fig. 9, *A1* and *A2*) and CA1 (Fig. 9, *B1* and *B2*) showed a distinct vulnerability to ischemia. By quantitative analysis, Fig. 9*C* reveals the total number of TUNEL-positive cells in the

postischemic motor cortex (23 ± 1.3/frame) was significantly lower than that in postischemic CA1 (113 ± 4.7/frame).

DISCUSSION

Using the monkey experimental paradigm, we demonstrate that Hsp70.1-BMP binding in the postischemic motor cortex contributes to an increase of ASM activity, thus promoting neuronal survival by inhibiting lysosomal destabilization or lysosomal rupture. On the other hand, failure of Hsp70-BMP binding in the postischemic CA1 contributes to a reduction of ASM activity, inducing lysosomal rupture and neuronal death. We provide several lines of evidence supporting the presence of Hsp70.1-BMP binding in the motor cortex and its absence in CA1 that differentially regulates ASM, and this affects neuronal cell fate after ischemia/reperfusion.

Hsp70.1 in Lysosomal Fraction and Its Localization—Following our protocol, we could not remove endoplasmic reticulum and the Golgi apparatus from the lysosomal fraction. Therefore, it is difficult to rule out the possibility that Hsp70.1 was up-regulated in other subcellular compartments, such as the endoplasmic reticulum, Golgi apparatus, and mitochondria.
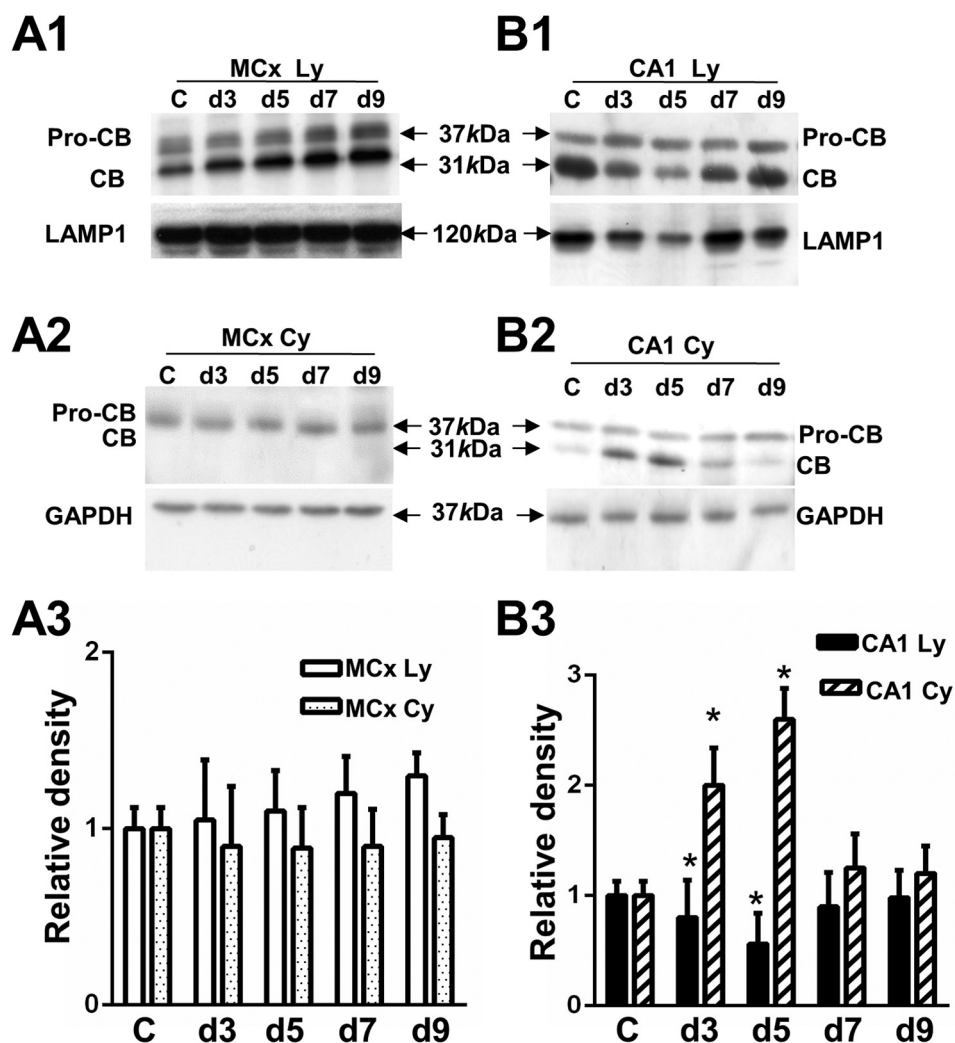
FIGURE 8. **Comparison of lysosomal stability between the postischemic motor cortex and CA1.** *A1* and *A2*, Western blot of cathepsin B in the enriched lysosomal (*MCx Ly*) and cytosolic fractions (*MCx Cy*) from the motor cortex. *B1* and *B2*, Western blot of cathepsin B in the enriched lysosomal (*CA1 Ly*) and cytosolic fractions (*CA1 Cy*) from the CA1. The protein levels of LAMP1 and GAPDH are shown as a loading control for lysosomal and cytosolic fractions, respectively. *Arrows*, proform cathepsin B (*pro-CB*) band at ∼37 kDa, mature cathepsin B (*CB*) band at ∼31 kDa, LAMP1 at 120 kDa, and GAPDH band at 37 kDa. *A3* and *B3*, densitometric analysis of cathepsin B proteins in the lysosome and cytosol from the motor cortex or the CA1 as compared with the non-ischemic control. *C*, non-ischemic control. *d3*, *d5*, *d7*, and *d9*, postischemic days 3, 5, 7, and 9. The values represent the mean ± S.E. of three independent experiment. *Asterisks* show significant difference from the non-ischemic control (*, $p < 0.05$).

Localization of Hsp70.1 on lysosomal membranes was confirmed by colocalization of Hsp70.1 and lysosomal membrane proteins, such as LAMP1 and CD63. The reduced LAMP1 (Figs. 1*D1* and 2*B2*) as well as a slight loss of CD63 in postischemic CA1 (Fig. 4*C2*) provoke the changes in lysosomal membrane localization of Hsp70.1, resulting in a low colocalization between Hsp70.1 and LAMP1 or CD63 in postischemic CA1 (Fig. 4, *C1* and *C2*).

Hsp70.1 Interaction with Lipids—Lipids and their metabolism may be particularly important for the brain due to their high concentrations, whereas the changes of lipid metabolism under stress conditions are involved in cerebral ischemic injury (24, 25). For example, the new mass spectroscopic technique MALDI MS revealed the changes of phospholipids, such as lysophosphatidylcholine, phosphatidylcholine, phosphatidyle-thanolamine, and sphingomyelin, in rat brains after focal cerebral ischemia (26). Studies have revealed that inducible Hsp70.1 has protective effects against ischemia and oxidative injury (27,

28); however, whether its protection correlates with membrane lipids remains to be elucidated. A recent study has demonstrated that Hsp70 selectively interacts with the negatively charged phospholipids, such as cardiolipin (CL), phosphatidyl-serine (PS), and BMP. Thus, Hsp70 attaches to the membranes abundant in the above lipids, including lysosomes, mitochondria, and the outer surface of cancer cells, without penetration (29). Accordingly, Hsp70 attaching to mitochondria containing CL exhibited the protection of membranes under stress conditions (30).

Hsp70 as the Substrate of Activated Calpain—Excessive activation of calpain and the resultant cleavage of substrate protein after ischemia/reperfusion have been reported to be related with neuronal death after cerebral ischemia (31–35). However, the *in vivo* substrate of activated μ-calpain was unknown. Using proteomics analysis by comparing the non-ischemic control and postischemic tissues from CA1, our group (15) identified oxidative modified proteins in postischemic CA1, showing ele-
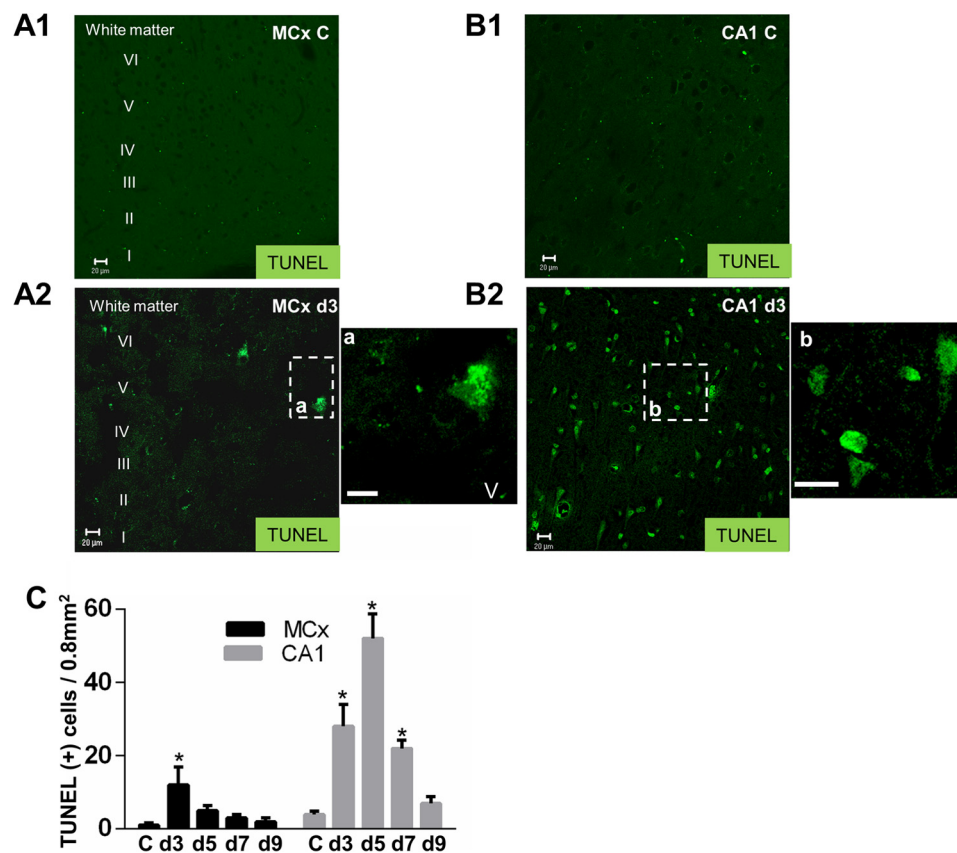
FIGURE 9. **Comparison of TUNEL staining between the postischemic motor cortex and CA1.** *A1* and *A2*, TUNEL staining in the non-ischemic motor cortex control (*MCx C*) and the postischemic motor cortex day 3 (*MCx d3*) (layer I through layer VI (*I–VI*)). *a* and *b*, *enlarged images* of the *boxed areas*. *B1* and *B2*, TUNEL staining in the non-ischemic CA1 control (*CA1 C*) and the postischemic CA1 day 3 (*CA1 d3*). *C*, representative quantitative analysis of TUNEL-positive cells in the motor cortex (*black bars*) and CA1 (*gray bars*) was done in grids of 800×1000 μm. *MCx*, motor cortex. *C*, the non-ischemic control. *d3*, *d5*, *d7*, and *d9*, postischemic days 3, 5, 7, and 9. The values represent the mean $\pm$ S.E. of three independent experiments. *Asterisks* show significant difference from the non-ischemic control (*, $p < 0.05$). All experiments were repeated three times with essentially similar results. *Scale bar*, 20 μm.

vated levels of carbonylated Hsp70.1 on postischemic days 3 and 5. Intriguingly, after the *in vitro* oxidative stresses induced by 4-hydroxy-2-nonenal, the non-ischemic monkey CA1 tissue showed calpain-mediated Hsp70.1 cleavage after its carbonylation, compared with the control (14), suggesting that oxidized Hsp70.1 may become a possible substrate of activated μ-calpain (36). Here we confirmed that activated μ-calpain was present at the lysosome of postischemic CA1 (Fig. 4*B*) but not in the postischemic motor cortex (Fig. 3*C*). We speculate that the *in vivo* substrate of μ-calpain is oxidized Hsp70.1. Because the N-terminal nucleotide binding domain and C-terminal substrate binding domain of Hsp70 are important for binding of lipids (29), we propose that normal biological functions of Hsp70.1 associated with the lipid binding domain may be disrupted, either by an oxidative modification of Hsp70.1 in the brains of early Alzheimer disease (37) or by calpain-mediated cleavage of oxidatively modified Hsp70.1 in the postischemic CA1 (11).

The BMP Levels and Oxidative Stress—The fatty acid composition of BMP is important for its biophysical properties. Bouvier *et al.* (38) found that the $C_{22:6}/C_{22:6}$ species of BMP was highly sensitive to oxidative stress, showing a significant decrease in macrophages after exposure to oxidative stresses, although many studies demonstrated the dramatic increase of BMP levels in the tissue of animals and humans with the lyso-

somal disorder, such as Niemann-Pick C disease, certain drug-induced lipidosis, and anti-phospholipid syndrome (39, 40). We carried out LC/MS analysis to measure the BMP levels, as compared with our current quantitative BMP measurement. The degradation of $C_{22:6}/C_{22:6}$ BMP by LC/MS was found in postischemic days 1 and 3 CA1 (41). Thus, the current measurement is equally suitable for the detection of BMP levels. These results indicate that degradation of BMP levels can increase oxidative stress, which causes modified (e.g. carbonylated) Hsp70.1 protein. Next, we also confirmed in *vivo* the levels of oxidative stress in the monkey brain, as measured by 4-hydroxy-2-nonenal immunoreactivity, a marker of oxidative stress. 4-Hydroxy-2-nonenal immunoreactivity could be not detected in the postischemic motor cortex (data not shown), whereas its immunoreactivity was markedly increased, showing a colocalization with Hsp70.1 (14), suggesting that high levels of oxidative stress occurred in the postischemic CA1 but not in postischemic motor cortex. The current study has suggested that oxidative stress aggravated brain injury in the hippocampal CA1 but not in the cortex of mice after the transient brain ischemia (42).

ASM and Ceramide Affect Lysosomal Stabilization and Neuronal Fate—Although *in vitro* cellular models are able to provide direct evidence in the Hsp70-mediated regulation of ASM activation, they cannot precisely reflect *in vivo* situations in
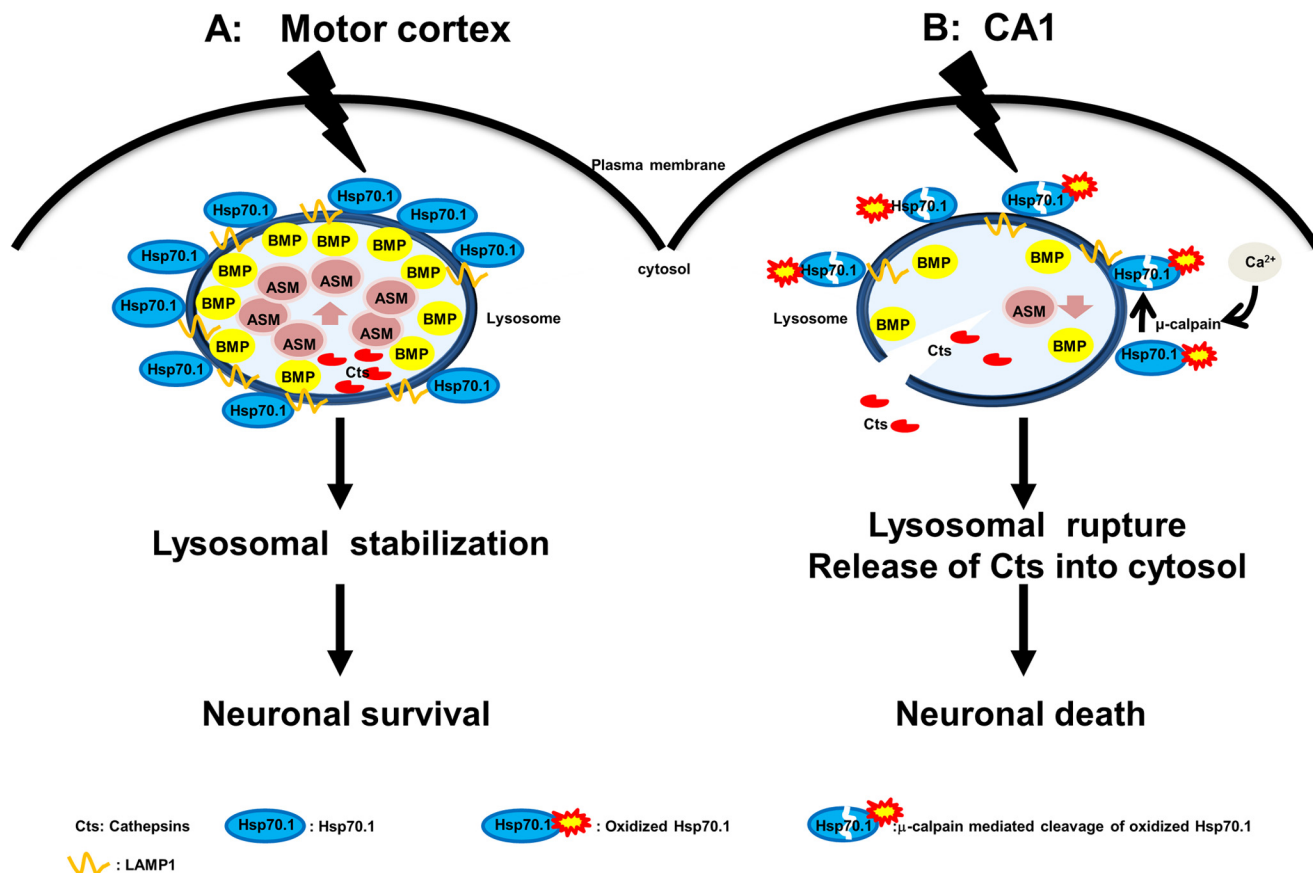
FIGURE 10. **The role of Hsp70.1 affecting neuronal fate by differentially regulating ASM.** *A*, in the postischemic motor cortex, up-regulated Hsp70.1 is present at lysosomal membranes and then binds to BMP, where μ-calpain activation and decreased BMP levels did not occur. Binding Hsp70.1 to BMP enhances ASM activity *in vivo* and facilitates lysosomal stabilization, resulting in protection of the motor cortex from neuronal cells death. *B*, in the postischemic CA1, cerebral ischemia causes μ-calpain activation and a concomitant reduction in both the lysosomal membrane localization of Hsp70.1 and BMP levels. Furthermore, the lipid binding domain of Hsp70 may be disrupted by activated μ-calpain-mediated cleavage of the oxidized Hsp70. Since this may diminish Hsp70-BMP binding, the resultant decrease in ASM activity *in vivo* may increase lysosomal rupture with leakage of cathepsin B into the cytosol and neuronal death.

brains with more complex nervous systems. The molecular events in the processing between the cellular models and the animal model of ischemia are distinct. Furthermore, ASM activity is known to occur transiently, peaking within a few min and declining within 1 h (9); thus, ASM activity in the monkey brain is difficult to analyze *in vivo.* Because BMP binding with ASM facilitates ASM activity (43), we reasoned that ASM-BMP binding (Fig. 7*B*) may represent *in vivo* increased ASM activity, as evidenced by an increase in expression of ASM proteins (Fig. 5, *A1*, *B11*, and *B12*) in the enriched lysosome fraction, lysosomal localization of ASM (Fig. 6*B*), and ASM-mediated generation of lysosomal ceramide (Fig. 7, *C* and *D2*) in postischemic day 3 motor cortex. A change in lipid composition of inner lysosomal membranes by an Hsp70-mediated increase in ASM activity was recently suggested to have a direct and potent influence on the stability of lysosomes (44).

In ischemic brain injuries and neurodegenerative diseases, activated ASM and elevated ceramide were coupled and translocated to the plasma membranes. However, in this study, ASM was localized inside lysosomes, and formation of lysosomal ceramide was not translocated to the plasma membranes (Fig. 7*D1*), suggesting that ASM and ceramide may have different effects on the cell survival or death, depending on the intracellular localization. In agreement with this concept, we found

that the neuronal fate in the postischemic motor cortex is distinct from that in the postischemic CA1 (Fig. 9). Based on these results, a hypothetical flow chart of neuronal cell fate is shown in Fig. 10.

REFERENCES

1. Schissel, S. L., Keesler, G. A., Schuchman, E. H., Williams, K. J., and Tabas, I. (1998) The cellular trafficking and zinc dependence of secretory and lysosomal sphingomyelinase, two products of the acid sphingomyelinase gene. *J. Biol. Chem.* **273,** 18250–18259
2. Kirkegaard, T., Roth, A. G., Petersen, N. H., Mahalka, A. K., Olsen, O. D., Moilanen, I., Zylicz, A., Knudsen, J., Sandhoff, K., Arenz, C., Kinnunen, P. K., Nylandsted, J., and Jäättelä, M. (2010) Hsp70 stabilizes lysosomes and reverts Niemann-Pick disease-associated lysosomal pathology. *Nature* **463,** 549–553
3. Petersen, N. H., Olsen, O. D., Groth-Pedersen, L., Ellegaard, A. M., Bilgin, M., Redmer, S., Ostenfeld, M. S., Ulanet, D., Dovmark, T. H., Lønborg, A., Vindeløv, S. D., Hanahan, D., Arenz, C., Ejsing, C. S., Kirkegaard, T., Rohde, M., Nylandsted, J., and Jäättelä, M. (2013) Transformation-associated changes in sphingolipid metabolism sensitize cells to lysosomal cell death induced by inhibitors of acid sphingomyelinase. *Cancer Cell* **24,** 379–393
4. Ellegaard, A. M., Groth-Pedersen, L., Oorschot, V., Klumperman, J., Kirkegaard, T., Nylandsted, J., and Jäättelä, M. (2013) Sunitinib and

SU11652 inhibit acid sphingomyelinase, destabilize lysosomes, and inhibit multidrug resistance. *Mol. Cancer Ther.* **12,** 2018 –2030

5. Saftig, P., and Sandhoff, K. (2013) Cancer: killing from the inside. *Nature* **502,** 312–313

6. Nylandsted, J., Gyrd-Hansen, M., Danielewicz, A., Fehrenbacher, N., Lademann, U., Høyer-Hansen, M., Weber, E., Multhoff, G., Rohde, M., and Jäättelä, M. (2004) Heat shock protein 70 promotes cell survival by inhibiting lysosomal membrane permeabilization. *J. Exp. Med.* **200,** 425– 435

7. Kirkegaard, T., and Jäättelä, M. (2009) Lysosomal involvement in cell death and cancer. *Biochim. Biophys. Acta* **1793,** 746 –754

8. Kolter, T., and Sandhoff, K. (2005) Principles of lysosomal membrane digestion: stimulation of sphingolipid degradation by sphingolipid activator proteins and anionic lysosomal lipids. *Annu. Rev. Cell Dev. Biol.* **21,** 81–103

9. Zeidan, Y. H., and Hannun, Y. A. (2010) The acid sphingomyelinase/ceramide pathway: biomedical significance and mechanisms of regulation. *Curr. Mol. Med.* **10,** 454 – 466

10. Yamashima, T. (2004) Ca^{2+}-dependent proteases in ischemic neuronal death: a conserved "calpain-cathepsin cascade" from nematodes to primates. *Cell Calcium* **36,** 285–293

11. Yamashima, T. (2012) Hsp70.1 and related lysosomal factors for necrotic neuronal death. *J. Neurochem.* **120,** 477– 494

12. Yamashima, T., Kohda, Y., Tsuchiya, K., Ueno, T., Yamashita, J., Yoshioka, T., and Kominami, E. (1998) Inhibition of ischaemic hippocampal neuronal death in primates with cathepsin B inhibitor CA-074: a novel strategy for neuroprotection based on "calpain-cathepsin hypothesis". *Eur. J. Neurosci.* **10,** 1723–1733

13. Yamashima, T. (2000) Implication of cysteine proteases calpain, cathepsin and caspase in ischemic neuronal death of primates. *Prog. Neurobiol.* **62,** 273–295

14. Sahara, S., and Yamashima, T. (2010) Calpain-mediated Hsp70.1 cleavage in hippocampal CA1 neuronal death. *Biochem. Biophys. Res. Commun.* **393,** 806 – 811

15. Oikawa, S., Yamada, T., Minohata, T., Kobayashi, H., Furukawa, A., Tada-Oikawa, S., Hiraku, Y., Murata, M., Kikuchi, M., and Yamashima, T. (2009) Proteomic identification of carbonylated proteins in the monkey hippocampus after ischemia-reperfusion. *Free Radic. Biol. Med.* **46,** 1472–1477

16. Zhu, H., Yoshimoto, T., Imajo-Ohmi, S., Dazortsava, M., Mathivanan, A., and Yamashima, T. (2012) Why are hippocampal CA1 neurons vulnerable but motor cortex neurons resistant to transient ischemia? *J. Neurochem.* **120,** 574–585

17. Yamashima, T., Saido, T. C., Takita, M., Miyazawa, A., Yamano, J., Miyakawa, A., Nishijyo, H., Yamashita, J., Kawashima, S., Ono, T., and Yoshioka, T. (1996) Transient brain ischaemia provokes Ca^{2+}, PIP2 and calpain responses prior to delayed neuronal death in monkeys. *Eur. J. Neurosci.* **8,** 1932–1944

18. Kikuchi, H., Imajoh-Ohmi, S., and Kanegasaki, S. (1993) Novel antibodies specific for proteolyzed forms of protein kinase C: production of anti-peptide antibodies available for *in situ* analysis of intracellular limited proteolysis. *Biochim. Biophys. Acta* **1162,** 171–176

19. Zinchuk, V., and Grossenbacher-Zinchuk, O. (2011) Quantitative colocalization analysis of confocal fluorescence microscopy images. *Curr. Protoc. Cell Biol.* 10.1002/0471143030.cb0419s39

20. Wei, J., Fujita, M., Nakai, M., Waragai, M., Sekigawa, A., Sugama, S., Takenouchi, T., Masliah, E., and Hashimoto, M. (2009) Protective role of endogenous gangliosides for lysosomal pathology in a cellular model of synucleinopathies. *Am. J. Pathol.* **174,** 1891–1909

21. Kobayashi, T., Stang, E., Fang, K. S., de Moerloose, P., Parton, R. G., and Gruenberg, J. (1998) A lipid associated with the antiphospholipid syndrome regulates endosome structure and function. *Nature* **392,** 193–197

22. Jenkins, R. W., Idkowiak-Baldys, J., Simbari, F., Canals, D., Roddy, P., Riner, C. D., Clarke, C. J., and Hannun, Y. A. (2011) A novel mechanism of lysosomal acid sphingomyelinase maturation: requirement for carboxyl-terminal proteolytic processing. *J. Biol. Chem.* **286,** 3777–3788

23. Linke, T., Wilkening, G., Lansmann, S., Moczall, H., Bartelsen, O., Weisgerber, J., and Sandhoff, K. (2001) Stimulation of acid sphingomyelinase activity by lysosomal lipids and sphingolipid activator proteins. *Biol. Chem.* **382,** 283–290

24. Adibhatla, R. M., and Hatcher, J. F. (2008) Altered lipid metabolism in brain injury and disorders. *Subcell. Biochem.* **49,** 241–268

25. Muralikrishna Adibhatla, R., and Hatcher, J. F. (2006) Phospholipase A2, reactive oxygen species, and lipid peroxidation in cerebral ischemia. *Free Radic. Biol. Med.* **40,** 376 –387

26. Shanta, S. R., Choi, C. S., Lee, J. H., Shin, C. Y., Kim, Y. J., Kim, K. H., and Kim, K. P. (2012) Global changes in phospholipids identified by MALDI MS in rats with focal cerebral ischemia. *J. Lipid Res.* **53,** 1823–1831

27. Chen, Z. C., Wu, W. S., Lin, M. T., and Hsu, C. C. (2009) Protective effect of transgenic expression of porcine heat shock protein 70 on hypothalamic ischemic and oxidative damage in a mouse model of heatstroke. *BMC Neurosci.* **10,** 111

28. Stetler, R. A., Gan, Y., Zhang, W., Liou, A. K., Gao, Y., Cao, G., and Chen, J. (2010) Heat shock proteins: cellular and molecular mechanisms in the central nervous system. *Prog. Neurobiol.* **92,** 184 –211

29. Mahalka, A. K., Kirkegaard, T., Jukola, L. T., Jäättelä, M., and Kinnunen, P. K. (2014) Human heat shock protein 70 (Hsp70) as a peripheral membrane protein. *Biochim. Biophys. Acta* **1838,** 1344 –1361

30. Polla, B. S., Kantengwa, S., François, D., Salvioli, S., Franceschi, C., Marsac, C., and Cossarizza, A. (1996) Mitochondria are selective targets for the protective effects of heat shock against oxidative injury. *Proc. Natl. Acad. Sci. U.S.A.* **93,** 6458 – 6463

31. Saido, T. C., Yokota, M., Nagao, S., Yamaura, I., Tani, E., Tsuchiya, T., Suzuki, K., and Kawashima, S. (1993) Spatial resolution of fodrin proteolysis in postischemic brain. *J. Biol. Chem.* **268,** 25239 –25243

32. Roberts-Lewis, J. M., Savage, M. J., Marcy, V. R., Pinsker, L. R., and Siman, R. (1994) Immunolocalization of calpain I-mediated spectrin degradation to vulnerable neurons in the ischemic gerbil brain. *J. Neurosci.* **14,** 3934 –3944

33. Neumar, R. W., Hagle, S. M., DeGracia, D. J., Krause, G. S., and White, B. C. (1996) Brain μ-calpain autolysis during global cerebral ischemia. *J. Neurochem.* **66,** 421– 424

34. Neumar, R. W., Meng, F. H., Mills, A. M., Xu, Y. A., Zhang, C., Welsh, F. A., and Siman, R. (2001) Calpain activity in the rat brain after transient forebrain ischemia. *Exp. Neurol.* **170,** 27–35

35. Bartus, R. T., Dean, R. L., Mennerick, S., Eveleth, D., and Lynch, G. (1998) Temporal ordering of pathogenic events following transient global ischemia. *Brain Res.* **790,** 1–13

36. Yamashima, T., and Oikawa, S. (2009) The role of lysosomal rupture in neuronal death. *Prog. Neurobiol.* **89,** 343–358

37. Sultana, R., Perluigi, M., Newman, S. F., Pierce, W. M., Cini, C., Coccia, R., and Butterfield, D. A. (2010) Redox proteomic analysis of carbonylated brain proteins in mild cognitive impairment and early Alzheimer's disease. *Antioxid. Redox Signal.* **12,** 327–336

38. Bouvier, J., Zemski Berry, K. A., Hullin-Matsuda, F., Makino, A., Michaud, S., Geloën, A., Murphy, R. C., Kobayashi, T., Lagarde, M., and Delton-Vandenbroucke, I. (2009) Selective decrease of bis(monoacylglycero)phosphate content in macrophages by high supplementation with docosahexaenoic acid. *J. Lipid Res.* **50,** 243–255

39. Hullin-Matsuda, F., Luquain-Costaz, C., Bouvier, J., and Delton-Vandenbroucke, I. (2009) Bis(monoacylglycero)phosphate, a peculiar phospholipid to control the fate of cholesterol: implications in pathology. *Prostaglandins Leukot. Essent. Fatty Acids* **81,** 313–324

40. Meikle, P. J., Whitfield, P. D., Rozaklis, T., Blacklock, D., Duplock, S., Elstein, D., Zimran, A., Mengel, E., Cannell, P., Hopwood, J. J., and Fuller, M. (2008) Plasma lipids are altered in Gaucher disease: biochemical markers to evaluate therapeutic intervention. *Blood Cells Mol. Dis.* **40,** 420 – 427

41. Yamashima, T. (2014) Calpain-mediated Hsp70.1 cleavage in monkey CA1 after ischemia induces similar "lysosomal vesiculosis" to Alzheimer neurons. *J. Alzheimers Dis. Parkinsonism* 10.4172/2161-0460.1000139

42. Yabuki, Y., and Fukunaga, K. (2013) Oral administration of glutathione improves memory deficits following transient brain ischemia by reducing brain oxidative stress. *Neuroscience* **250,** 394 – 407

43. Linke, T., Wilkening, G., Sadeghlar, F., Mozcall, H., Bernardo, K., Schuchman, E., and Sandhoff, K. (2001) Interfacial regulation of acid ceramidase activity. Stimulation of ceramide degradation by lysosomal lipids and sphingolipid activator proteins. *J. Biol. Chem.* **276,** 5760 –5768

44. Petersen, N. H., Kirkegaard, T., Olsen, O. D., and Jäättelä, M. (2010) Connecting Hsp70, sphingolipid metabolism and lysosomal stability. *Cell Cycle* **9,** 2305 –2309